Observation of excited states in the near-drip-line nucleus ^{125}Pr

A. N. Wilson,[1] D. R. LaFosse,[2] J. F. Smith,[3] C. J. Chiara,[2,4] A. J. Boston,[5] M. P. Carpenter,[6] H. J. Chantler,[5] R. Charity,[4]
P. T. W. Choy,[5] M. Devlin,[4] A. M. Fletcher,[3] D. B. Fossan,[2] R. V. F. Janssens,[6] D. G. Jenkins,[5,*] N. S. Kelsall,[7]
F. G. Kondev,[6] T. Koike,[2] E. S. Paul,[5] D. G. Sarantites,[4] D. Seweryniak,[6] K. Starosta,[2] and R. Wadsworth[7]

[1]*Department of Nuclear Physics, Research School of Physical Sciences and Engineering, Australian National University,
Canberra ACT 0200, Australia*
[2]*Department of Physics and Astronomy, State University of New York at Stony Brook, Stony Brook, New York 11794-3800*
[3]*Schuster Laboratory, The University of Manchester, Manchester M13 9PL, United Kingdom*
[4]*Department of Chemistry, Washington University, St. Louis, Missouri 63130*
[5]*Oliver Lodge Laboratory, The University of Liverpool, Liverpool L69 7ZE, United Kingdom*
[6]*Argonne National Laboratory, Argonne, Illinois 60439*
[7]*Department of Physics, University of York, Heslington, York YO10 5DD, United Kingdom*
(Received 20 March 2002; published 23 August 2002)

High-spin states have been observed in the near-drip-line nucleus ^{125}Pr following the reaction ^{64}Zn(^{64}Zn,$p2n$). The detection of charged particles and neutrons evaporated from the compound system, along with the M/q of the recoiling nucleus, have allowed the identification of excited states in ^{125}Pr and the unambiguous assignment of five rotational structures to this nucleus. This is the most neutron-deficient Pr isotope in which excited states have been observed. The strongest band is identified as the $h_{11/2}$ single-quasiproton configuration, and is observed to a maximum spin of $I=(67/2\hbar)$. Another structure is interpreted as the $g_{9/2}$ proton hole state, which is associated with bands of enhanced deformation observed in several nuclei in this mass region. These two bands are compared with analogous bands in the heavier odd-A Pr isotopes and changes in deformation are discussed.

Extremely neutron-deficient nuclei with mass $A \approx 130$ can be populated (albeit with low cross sections) in heavy-ion fusion-evaporation reactions using stable beam/target combinations. Such reactions, when studied with large arrays of Ge detectors coupled to efficient particle-detection systems, allow nuclei very close to and even at the proton drip line to be studied at high spins. For $Z=59$ (Pr isotopes), the drip line has been predicted to lie at ^{126}Pr [1,2] and more recently at ^{124}Pr [3]—to date, the most neutron-deficient Pr isotope in which excited states have been observed is ^{126}Pr [4,5]. The isotope ^{125}Pr has previously been identified in a mass-separation experiment by its β^+ decay to ^{125}Ce [6]; the half-life of the ground state was measured as 3.3 s, but no excited states or γ-ray decays were observed. In the present work, γ-ray transitions have been observed to high spins in ^{125}Pr. The data were obtained using the Gammasphere γ-ray detector array [7], in conjunction with both neutron and charged-particle detectors and a recoil mass separator which allowed the assignment of five rotational bands to ^{125}Pr. This work focuses on the identification of these structures, and on the evidence concerning deformation trends provided by two bands identified as corresponding to the $h_{11/2}$ and $g_{9/2}$ single-quasiproton excitations. A more comprehensive presentation of the level scheme will be given in a forthcoming publication [8].

In the Pr isotopes, the specific orbitals occupied in low-lying configurations and the nuclear deformations are strongly interdependent. The lowest-lying states are associ-ated with single-quasiproton $\pi d_{5/2}$ and $\pi g_{7/2}$ configurations. At low spins, excitations into $\pi h_{11/2}$ levels, which give rise to decoupled bands, occur at moderate deformations ($\beta_2 \approx 0.25$), while $\pi g_{9/2}$ hole excitations resulting in characteristic pairs of strongly coupled signature-partner bands occur at values of β_2 close to superdeformation in this region ($\beta_2 \approx 0.4$). In fact, rotational bands associated with *enhanced deformations* ("ED" bands) have been observed in many nuclei with $A \approx 130$. Initially, it was thought that the adoption of large deformations in this region was due to the presence of $i_{13/2}$ neutron ($\nu i_{13/2}$) intruder orbitals close to the Fermi level. However, the observation of such structures in $^{127-131}$Pr [9–11] and ^{133}Pm [12] revealed that the $\pi g_{9/2}$ configuration may also produce very elongated nuclear shapes, as, in these cases, the $\nu i_{13/2}$ levels are far from the Fermi surface and cannot contribute to the deformation.

Although the low-lying states in the odd-A Pr isotopes are dominated by single-quasiproton excitations, the character of the neutron orbitals close to the Fermi level will also influence the nuclear shape. For $N=70-72$, $(d_{5/2}g_{7/2})$, $d_{3/2}$, and midshell $h_{11/2}$ levels are expected to be close to the Fermi level at $\beta_2 \approx 0.25$, making a small or negative contribution to the deformation of the $\pi h_{11/2}$ state. Larger deformations bring the deformation-driving $\nu[541]1/2$ intruder orbital [originating from the $\nu(h_{9/2}f_{7/2})$ shell] close to the Fermi level. It has been suggested [13] that this orbital plays an additional role in supporting the ED states in $^{127-131}$Pr, and that the large deformation is not solely due to the $\pi g_{9/2}$ level. For smaller values of N, different neutron orbitals come into play for both $\pi h_{11/2}$ and $\pi g_{9/2}$ states. At moderate deformations, $\nu h_{11/2}$ orbitals become available which will tend to

increase the total deformation. Thus one expects to see an increasing deformation associated with the $\pi h_{11/2}$ state, with a maximum predicted at $N=64$. On the other hand, the lowering of the neutron Fermi level at larger deformations results in a decreasing influence for the $\nu(h_{9/2} f_{7/2})$ intruder. As N decreases this level becomes increasingly distant from the Fermi level, and so its contribution to the deformation of the $\pi g_{9/2}$ hole state will gradually disappear. At some value of N, the occupation probability of this orbital, and hence its effect on the deformation, will be negligible; it will then be possible to isolate the contribution to the enhanced deformation arising from the $\pi g_{9/2}$ hole. In the current work, bands have been observed in ^{125}Pr ($N=66$) which are assigned the $\pi h_{11/2}$ and $\pi g_{9/2}$ configurations. The data indicate that the deformation associated with the former is larger than in the $N=68$ neighbor, while that associated with the latter is unchanged.

An experiment was performed to study these nuclei using the ^{64}Zn(^{64}Zn) reaction. The beam, supplied by the ATLAS accelerator at an energy of 260 MeV, was incident upon a thin (500 μg/cm^2) ^{64}Zn target. Gamma rays were detected using 78 Ge detectors of the Gammasphere array. Protons and α particles evaporated from the recoiling nuclei were detected using the Microball [14] array; neutrons were detected by the Neutron Shell (an array of 30 NE213 scintillators provided by Washington University, St. Louis). Mass-to-charge-state ratios, M/q, of recoiling evaporation residues were measured by the Argonne fragment mass analyzer (FMA) [15] for $\approx$75% (3 d) of the beam time. A total of $\sim 1 \times 10^9$ events were recorded in which either $\geq 3\gamma$ rays or $\geq 2\gamma$ rays plus either a recoil or a neutron were detected.

In order to select out the $1p2n$ evaporation channel leading to ^{125}Pr from the overwhelming majority of other reaction channels, charged-particle (p, α) and neutron (n) detection requirements were imposed. Initially, a series of matrices was created with varied conditions on the number of each type of coincident particle. It was found that scattering between the scintillator detectors led to a significant leak-through of $(x-1)n$ events into xn-gated spectra. This problem was much reduced by suppressing neighboring elements of the Neutron Shell and gating on the resulting neutron fold. In this paper, neutron folds henceforth refer to numbers after suppression.

With an effective efficiency of $\sim$50%, leak-through from $2n$ to $1n$ channels was also significant (the "raw" efficiency is $\approx$30%: the increase is due to the trigger conditions); however, the $p3n$ channel has a negligible cross section in this reaction, and thus did not contaminate the $p2n$-gated spectra. Gamma rays were therefore assigned to ^{125}Pr using spectra gated by exactly two neutrons. Leak-through from higher particle-fold events also occurred in the charged-particle gates, due to the efficiency of the Microball array ($\sim$80% for proton detection and $\sim$65% for α detection). Thus yp-gated spectra contained a fraction of $(y+1)p$ events, and smaller contributions from higher-fold p and α channels. The cross section for the production of Pr isotopes in this reaction is much smaller than that for the production of Ce isotopes, reached by $2pxn$ emission, and so peaks associated with $2p$ events dominate the $1p$-gated spectra. Figure 1(a) shows the total projection of a $1p2n$-gated matrix; the most intense peaks arise from the $2p2n$ channel to ^{124}Ce. There are also peaks associated with ^{125}Ce ($2p1n$), indicating that some $1n$ events remain even after nearest-neighbor suppression.
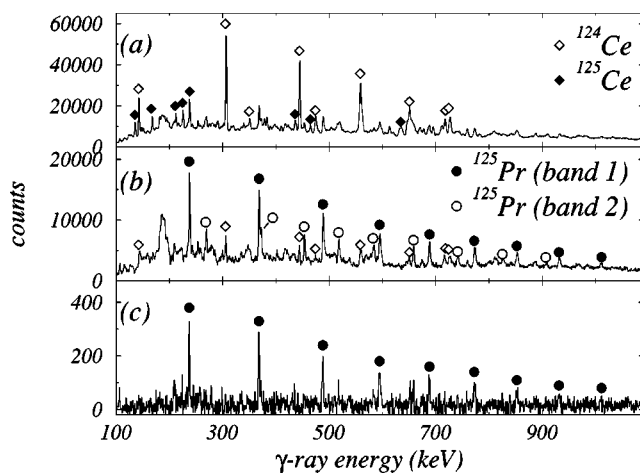

FIG. 1. (a) Total projection of the $1p2n$-gated matrix. (b) Results of subtracting a fraction of the $2p2n$-gated matrix from the $1p2n$-gated matrix. (c) Spectrum gated by the detection of a recoil of mass $A=125$, one proton, and one or two neutrons. A fraction of the $A=125$, $2p1n$ spectrum has been subtracted. The legends refer to all panels.
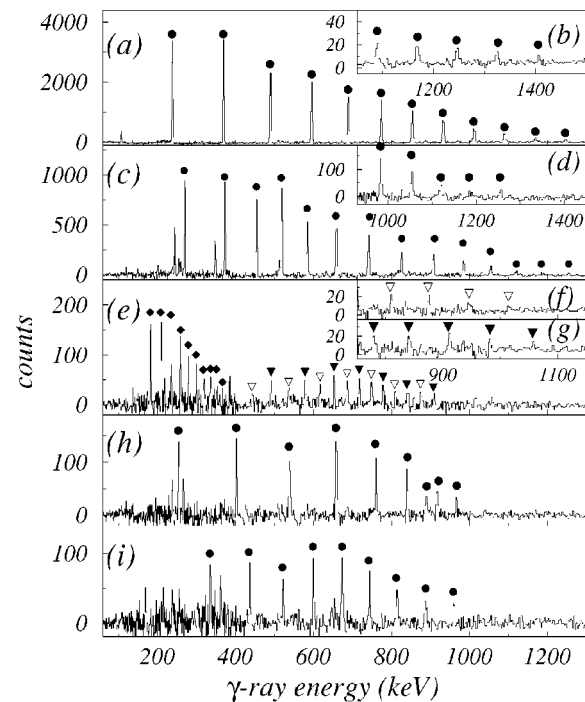

FIG. 2. Double-gated spectra projected from the $1p \geq 1n$-gated cube showing (a) band 1 and (b) the high-energy portion of band 1; (c) band 2 and (d) the high-energy portion of band 2; (e) band 3 and (f) and (g) the high-energy portions of the two signatures of band 3; (h) band 4; and (i) band 5. All clean combinations of pairs of gates were used to create the spectra shown in the main panels; combinations enhancing the high-energy peaks were used for panels (b), (d), (f), and (g).
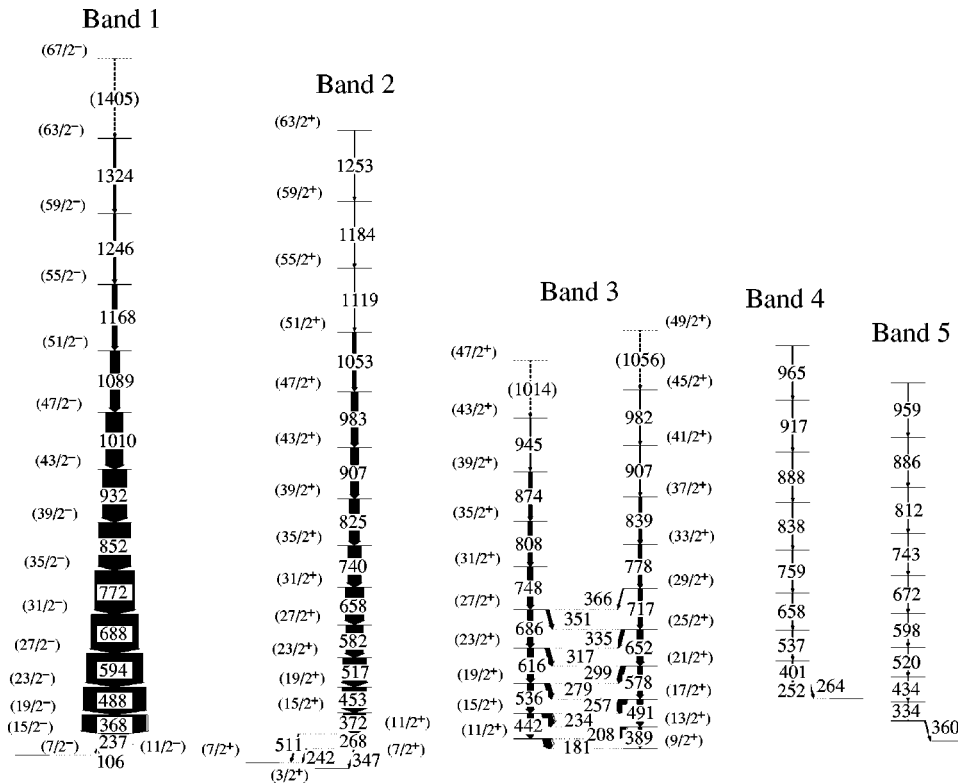
FIG. 3. The high-spin level scheme of ^{125}Pr constructed in this work.

Figure 1(b) shows the spectrum produced after subtracting a fraction of a $2p2n$-gated matrix. This second matrix contains leak-through from higher p-fold and α events and so provides a reasonable approximation to the Microball leak-through background in the $1p2n$ gate. Although some $2p$ data remains, both ^{124}Ce and ^{125}Ce have been the subject of thorough studies [16] and so γ rays from these nuclei can be identified as such. None of the structures previously observed in ^{126}Pr [4,5] were observed in this matrix, allowing the $1p1n$ channel to be eliminated as the source of any γ rays. Each of the unknown peaks in the total projection was then selected in turn and the associated coincidence relationships investigated. This led to the identification of five rotational structures which have been assigned to ^{125}Pr. These structures were searched for in matrices produced with gates set on nonzero α and higher p and n folds; no evidence was found for them in any of these spectra.

Spectra were also created gated by the M/q data provided by the FMA. The spectrum shown in Fig. 1(c) is gated by $A = 125$ and $1p(1,2)n$. A fraction of the spectrum gated by $A = 125$ and $2p(1,2)n$ has been subtracted to remove the strongly populated leak-through nucleus ^{125}Ce. Because of the relatively low efficiency of the FMA ($\sim 3\%$), only the strongest of the structures observed in the $1p2n$-gated data are visible; however, the confirmation of the mass of the nucleus provides an additional verification of ^{125}Pr.

A three-dimensional array (cube) suitable for analysis using the RADWARE package [17] was also created, incremented with unpacked triple γ coincidences gated by $1p \geqslant 1n$. This was used to further investigate the structures already assigned to ^{125}Pr using the procedures described above. As an additional means of verifying the assignment,

the ratio of the intensity of the bands in this cube to their intensity in an ungated cube was compared to the same ratio for structures associated with other reaction products. In each case, the intensity of a single clean double gate was measured in both cubes. The bands assigned to ^{125}Pr all result in a ratio of 0.45. The bands associated with contaminant channels were significantly more diminished; for example, the ratio obtained for the $2p2n$ channel ^{124}Ce was 0.19, that for the $2p1n$ channel ^{125}Ce is 0.10, and that for the $3p2n/\alpha p$ channel ^{123}La is 0.01. Spectra of the five structures, projected from the gated cube, are shown in Fig. 2.

Finally, γ-γ matrices were sorted in order to extract angular distribution information where possible. The resulting level scheme is presented in Fig. 3. Suggestions for band-head spins for bands 1, 2, and 3 come from comparison with analogous bands in heavier odd-A Pr isotopes. Detailed results concerning all five bands will be presented in a separate publication; this work concentrates on information concerning the *deformations* associated with bands 1 and 3.

Band 1 is a decoupled band for which no signature partner has been found. It was populated with the most intensity of the five bands assigned to ^{125}Pr and therefore is most likely to be based on the low-spin yrast configuration, i.e., the favored signature of the $\pi h_{11/2}$ orbital. A plot of the aligned angular momentum i_x of band 1 as a function of rotational frequency is shown in Fig. 4(a); the dynamic moment of inertia $\mathcal{J}^{(2)}$ is shown in Fig. 4(b). Data for the bands identified as being based on the $\pi h_{11/2}$ orbital in the heavier odd-Z isotopes ^{127,129,131}Pr [9,10,18] are included in the figure. Harris parameters of $J_0 = 17.0\hbar^2/\text{MeV}, J_1 = 25.8\hbar^4/\text{MeV}^3$ have been employed to facilitate comparison among the
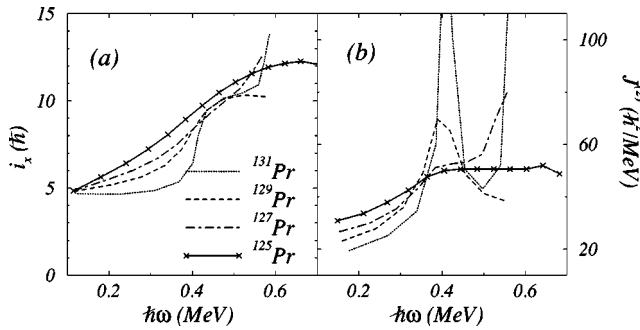
FIG. 4. Plots of (a) the aligned angular momentum i_x and (b) the dynamic moment of inertia $\mathcal{J}^{(2)}$ extracted for band 1 in ^{125}Pr and the analogous bands in ^{127,129,131}Pr. The legend applies to both panels.
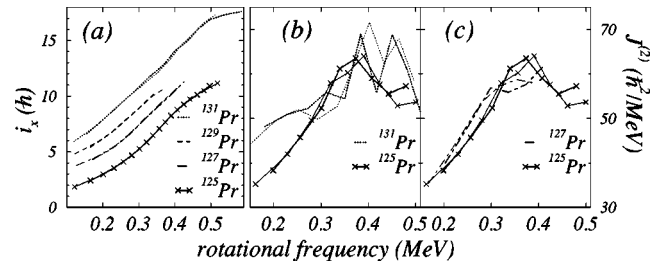

FIG. 5. The (a) aligned angular momenta i_x and (b) and (c) dynamic moments of inertia $\mathcal{J}^{(2)}$ of the $\alpha = \pm 1/2$ signatures of band 3 (bold/faint unbroken lines) and the analogous bands in ^{131,129,127}Pr (dotted, dashed, and dot-dashed lines, respectively). The i_x values for ^{131,129,127}Pr have been offset by $4\hbar$, $3\hbar$, and $2\hbar$ for clarity.

bands; these parameters have been widely used in this mass region and are found to give reasonable results for many nuclei.

The alignment of the first $\pi h_{11/2}$ pair has been observed at $\hbar\omega = 0.27$ MeV in the bands assigned to $\pi g_{7/2}$ excitations in the heavier Pr isotopes [9,10,18] and also in band 2 in this nucleus, which is assigned the $g_{7/2}$ configuration [8]. There is no evidence for this alignment in band 1, supporting the suggestion that it represents a configuration in which one of the signatures of this pair is occupied. There is a steady gain in alignment over most of the observed frequency range; a comparison with the heavier Pr isotopes reveals a clear trend in that, as N decreases, the observed increase becomes more gradual, changing from a sharp upbend to a smooth rise. The change in the shape of the i_x curves may be contributed to by the use of a fixed reference which does not reflect changes in deformation. However, the $\mathcal{J}^{(2)}$ curves shown in Fig. 4(b) confirm that an interaction is taking place in all four nuclei around $\hbar\omega \approx 0.4$ MeV, and that there is a marked change in the character of the interaction. The underlying cause of this interaction, in these and neighboring nuclei, is a matter of some debate, with alternative interpretations as the first $h_{11/2}$ quasineutron alignment [9,10,19–21] or the first *unblocked* $h_{11/2}$ quasiproton alignment [11,22]. The question of the nature of the alignment gain in band 1 in ^{125}Pr is outside the domain of the present paper, which addresses trends in the deformations associated with $\pi h_{11/2}$ and $\pi g_{9/2}$ structures at low spins, and will be discussed in the context of detailed calculations in a separate publication. The observed properties of this band are sufficient to allow an assignment to the $\pi h_{11/2}$ configuration at low spin, and therefore to allow comparison with the $\pi h_{11/2}$ bands in the heavier isotopes below the alignment.

Inspection of Fig. 4 shows that the $\mathcal{J}^{(2)}$ moment of band 1 continues a trend of increasing magnitude with decreasing N. The initial magnitude is $\approx 19\hbar^2$/MeV in ^{131}Pr; each lighter isotope shows an increase, until the magnitude is $\approx 30\hbar^2$/MeV in ^{125}Pr. This pattern may be indicative of an increase in the associated deformation. Total Routhian surface (TRS) calculations [23,24] have been performed which indicate an increase in the deformation associated with the $\pi h_{11/2}$ state from $\beta_2 = 0.256$ in ^{131}Pr (slightly larger than indicated by the measured lifetime [10]) to $\beta_2 = 0.299$ in

^{125}Pr, which is only 10% smaller than the measured deformation of the ED band in ^{131}Pr. Such an increase would be expected to result in a corresponding increase in the overall magnitude of the $\mathcal{J}^{(2)}$, as indeed is observed experimentally. This supports the suggestion that the deformation associated with this state is larger than in the heavier isotopes.

Band 3 consists of two cascades linked by strong interband transitions up to spin $I = (29/2\hbar)$. For reasonable nuclear deformations, the $\pi g_{9/2}$ orbital is the only available excitation which would result in such a structure and band 3 is therefore assigned this configuration. The i_x values extracted for this band are shown in Fig. 5(a), along with values for the analogous bands in ^{127,129,131}Pr [10,9,13]. Each curve exhibits a steady increase up to $\hbar\omega \approx 0.51$ MeV, although the band in ^{131}Pr experiences a larger total gain. However, as was suggested above, such differences may be due to the subtraction of the same reference in all isotopes. The $\mathcal{J}^{(2)}$ of band 3 is also shown in Fig. 5 in comparison with the bands in ^{131}Pr [Fig. 5(b)] and ^{127}Pr [Fig. 5(c)]. A comparison with the band in ^{129}Pr is omitted as it is not observed through the interaction region.

Galindo-Uribarri *et al.* observed the beginning of an interaction in the $\pi g_{9/2}$ band in ^{131}Pr at $\hbar\omega \approx 0.39$ MeV [10]. Subsequent work [13] extended both signatures of this band, and although the behavior is rather peculiar, possibly indicating two interactions, it appears that a first crossing is experienced at $\hbar\omega \approx 0.4$ MeV at the earliest [see Fig. 5(b)]. This is interpreted as the $\pi h_{11/2}$ crossing, occurring $\hbar\omega \approx 0.13$ MeV higher than in the $\pi g_{7/2}$ band [10]. In ^{131}Pr, the deformation of the $\pi g_{7/2}$ state is expected to be similar to that of the $\pi h_{11/2}$ state, and thus much less than that of the $g_{9/2}$ state. Higher-K substates will be closer to the Fermi level for the ED state, resulting in the observed difference in alignment frequencies. The interaction occurring in band 3 in ^{125}Pr is most likely to be due to the same $h_{11/2}$ quasiproton alignment. However, although there are gross similarities between the $\pi g_{9/2}$ bands in these two nuclei, there are also significant differences. The interaction in band 3 occurs at a lower frequency ($\hbar\omega \approx 0.38$ MeV), and the overall magnitude of the $\mathcal{J}^{(2)}$ is lower, particularly at low frequencies before the alignment takes place. Both of these features indicate a smaller deformation, as would be expected if the $\nu(h_{9/2}f_{7/2})$ orbital makes a greater contribution to the deformation of the heavier isotope.

Figure 5(c) shows that the behavior of band 3 is much like that of the $\pi g_{9/2}$ band in ^{127}Pr. The initial magnitudes of the $\mathcal{J}^{(2)}$ moments are the same and the interaction appears to occur at the same frequency in both nuclei. These similarities suggest that there is little or no difference between the deformations associated with the $\pi g_{9/2}$ bands in these nuclei, i.e., that the lowering of the Fermi level from $N=68$ to $N=66$ has little effect. (This suggestion of similar deformations is consistent with the TRS calculations for positive parity configurations in the two nuclei.) This indicates that the limit of the influence of the $(h_{9/2}f_{7/2})$ neutron orbital may have been reached and that the deformation of the band in ^{125}Pr may be attributable to the influence of the $\pi g_{9/2}$ hole alone.

A direct comparison of the characteristics of bands 1 and 3 may also be made. As was noted above, the initial magnitude of the $\mathcal{J}^{(2)}$ moment of band 1 is approximately $30\hbar^2$/MeV. That associated with band 3 is approximately $35\hbar^2$/MeV at the lowest observed frequency. The difference is small, particularly when compared to the variations seen over the isotope chain for the $\pi h_{11/2}$ bands. If the increased $\mathcal{J}^{(2)}$ moment of the $\pi h_{11/2}$ band is taken as a reflection of an increased deformation, the similarity in the magnitudes of the moments of the two bands in ^{125}Pr may also suggest that the deformation associated with the $\pi g_{9/2}$ configuration is not significantly enhanced relative to the $h_{11/2}$ configuration in ^{125}Pr. On the other hand, the $\pi h_{11/2}$ alignment frequency in band 3 is ≥ 0.1 MeV/$\hbar$ higher than in the $g_{7/2}$ bands in both this and the heavier isotopes, suggesting that the difference in deformation associated with these two structures remains large. Thus it may be that both the $h_{11/2}$ and $g_{9/2}$ qua-

siproton structures may be associated with "enhanced" deformations relative to the $g_{7/2}$ and ground-state structures. Lifetime measurements yielding quadrupole moments are necessary to determine the answers to these questions.

In conclusion, the powerful combination of the Gammasphere, Microball, and Neutron Shell detector arrays, in conjunction with the FMA, have allowed five rotational structures to be identified in the near-drip-line nucleus ^{125}Pr. This is the most neutron-deficient Pr isotope in which excited states have been observed. Two of the most intensely populated of these structures, bands 1 and 3, have been assigned single-quasiproton $\pi h_{11/2}$ and $\pi g_{9/2}$ configurations, respectively. Band 1 continues the trend observed in heavier Pr isotopes of apparently increasing interaction strength at the first alignment with decreasing N, along with increasing $\mathcal{J}^{(2)}$. It is suggested that this behavior reflects an increasing deformation.

The results obtained for the $\pi g_{9/2}$ band do not continue the trend of decreasing $\mathcal{J}^{(2)}$ and $\pi h_{11/2}$ alignment frequency. Comparison with ^{127}Pr reveals very little difference between the $g_{9/2}$ bands in these two nuclei. This indicates that the deformation of this state is not contributed to by the $(h_{9/2}f_{7/2})$ neutron intruder orbital. This is the first time it has been possible to isolate the contribution of the $\pi g_{9/2}$ state to the deformation of the ED bands in the Pr isotopes.

[1] M. Beiner, R.J. Lombard, and D. Mass, At. Data Nucl. Data Tables **17**, 450 (1976).

[2] G. Audi and A.H. Wapstra, Nucl. Phys. **A565**, 66 (1993).

[3] D. Vretenar, G.A. Lalazissis, and P. Ring, Phys. Rev. Lett. **82**, 4595 (1999).

[4] D.J. Hartley *et al.*, Phys. Rev. C **63**, 041301(R) (2001).

[5] C.M. Petrache *et al.*, Phys. Rev. C **64**, 044303 (2001).

[6] A. Osa, M. Asai, M. Koizumi, T. Sekine, S. Ichikawa, Y. Kjima, H. Yamamoto, and K. Kawade, Nucl. Phys. **A588**, 185c (1995).

[7] P.J. Nolan, F.A. Beck, and D.B. Fossan, Annu. Rev. Nucl. Part. Sci. **45**, 561 (1994).

[8] A. N. Wilson *et al.* (unpublished).

[9] S.M. Mullins *et al.*, Phys. Rev. C **58**, R2626 (1998).

[10] A. Galindo-Uribarri *et al.*, Phys. Rev. C **50**, R2655 (1994).

[11] P.K. Weng *et al.*, Phys. Rev. C **47**, 1428 (1993).

[12] A. Galindo-Uribarri *et al.*, Phys. Rev. C **54**, 1057 (1996).

[13] B.H. Smith, L.L. Riedinger, H.Q. Jin, W. Reviol, W. Satula, A. Galindo-Uribarri, D.G. Sarantites, J.N. Wilson, D.R. LaFosse, and S.M. Mullins, Phys. Lett. B **443**, 89 (1998).

[14] D.G. Sarantites *et al.*, Nucl. Instrum. Methods Phys. Res. A

381, 418 (1996).

[15] C.N. Davids, B.B. Back, K. Bindra, D.J. Henderson, W. Kutschera, T. Lauritsen, Y. Nagame, P. Sugathan, A.V. Ramayya, and W.B. Walters, Nucl. Instrum. Methods Phys. Res. B **70**, 358 (1992).

[16] J. F. Smith *et al.* (unpublished).

[17] D.C. Radford, Nucl. Instrum. Methods Phys. Res. A **361**, 297 (1995).

[18] A. Galindo-Uribarri *et al.*, Atomic Energy of Canada Ltd, Report No. AECL-11132 PR-TASCC-09, 1994.

[19] R. Wyss, F. Liden, J. Nyberg, A. Johnson, D.J.G. Love, A.H. Nelson, D.W. Banes, J. Simpson, A. Kirwan, and R. Bengtsson, Nucl. Phys. **A503**, 244 (1989).

[20] C.M. Parry *et al.*, Phys. Rev. C **57**, 2215 (1998).

[21] A.N. Wilson *et al.*, Phys. Rev. C **63**, 054307 (2001).

[22] D.J. Hartley *et al.*, Phys. Rev. C **65**, 044329 (2002).

[23] W. Nazarewicz, J. Dudek, R. Bengtsson, and I. Ragnarsson, Nucl. Phys. **A435**, 397 (1985).

[24] S. Cwiok, J. Dudek, W. Nazarewicz, W. Skalski, and T. Werner, Comput. Phys. Commun. **46**, 379 (1987).